Adaptive triggering for scintillation signals

J. Vesic[1], M. Vencelj[1], K. Strnisa[2], D. Savran[3]

[1] Jozef Stefan Institute, Ljubljana, Slovenia
[2] Cosylab d.d., Ljubljana, Slovenia
[3] EMMI, GSI, Darmstadt, Germany; FIAS, Frankfurt am Main, Germany

E-mail: jelena.vesic@ijs.si

Abstract. Due to the stochastic nature of the pulse creation in a scintillation detector the output pulses are not all of the same shape but rather 'noised' with statistical fluctuations on the pulse tails, which may induce false triggers. The current state of the art in solving this kind of problems is either introducing a deadtime after each pulse which makes the detector inefficient at higher count rates or raising the trigger threshold above the fluctuactions level, which on the other side, lowers the dynamic range of the detector from the low energy side. In order to meet the ever growing demand for high precision/efficient experiments the solutions to these limitations are highly desirable. We propose a new method, the adaptive triggering for scintillation signals.

1. Introduction

Scintillation detectors will be an important part of detection systems in FAIR (Facility for Antiproton and Ion Research). In order to extract maximum information from the scintillation pulses, improved signal processing is required.
Precision of signal magnitude is limited by fluctuations. We can differ between two types of fluctuations. The first one are the fluctuations due to the stohastic nature of the pulse creation and the second are the baseline fluctuations due to the electronics. Main contribution to the fluctuations in the scintillator signals originates from the statistical fluctuations. Namely, the output pulses are not all the same shape but noised with statistical fluctuations on the pulse tails, which give rise to the afterpulsing. However, we have to note that some non-statistical processes also can give rise to the afterpulsing, namely the emission of light from the latter stages of the multiplier structure which finds its way back to the photocatode [1]. Also, another cause of afterpulsing can be an imperfect vacuum within the tube. Residual gas can be ionized by the passage of electrons through the multiplier structure. Formed positive ions will drift in the reverse direction and eventually some may find a path back to the photocatode [1].
The pulses from the scintillation detectors have exponential shapes. The main role of the signal processing that happens afterwards is to create a pulse which amplitude is proportional to the deposited energy. In the traditional analog pulse shaping, a combination of two basic filters has been used, namely CR and RC filters. The CR filter is a high pass filter and it allows only high frequency components of the pulse to pass, blocking the DC component of the signal. An integrator is a low pass filter, it only passes the low frequency components of the signal and modifies the differentiated pulse

by widening its maximum. However if the original exponential pulse is noised with statistical fluctuations, the semigaussian processed signal will have the statistical fluctuations as well, which might cause detection of false pulses or the information on amplitude value not correctly deduced. One of the digital processing methods (DSP) that is commonly used is a moving window deconvolution method (MWD) [2, 3]. We chose DSP over the analog processing mainly due to its flexibility (simple to change filter parameters etc.).

In our experiment, signal from a photomultiplier tube (PMT) was firstly sampled with a fast digitizer to reconstruct the pulse and the MWD method was used consequently for the offline DSP. The concept of the MWD method is similar to the analog pulse shaping. The output of a PMT is a fast rising step followed by an exponential relaxation. In order to be able to measure its amplitude, it is favorable to reshape signal to a more readable form. One of the algorithms for shaping it is the MWD algorithm. The single exponential decay with an initial time t=0 and decay time τ is written as:

$$f(t) = \begin{cases} Ae^{-t/\tau}, & t \geq 0 \\ 0. & t < 0 \end{cases} \quad (1)$$

Knowing the value $f(t_n)$ at time t_n, the initial amplitude can be found as:

$$A = f(t_n) + A - f(t_n) = f(t_n) + A\left(1 - e^{-\frac{t_n}{\tau}}\right) = f(t_n)\frac{\int_0^{t_n} f(t)dt}{\tau}. \quad (2)$$

In order to use the previous equation in digital domain, it should be written in a discrete form:

$$A[n] = x[n] + \frac{\sum_{k=0}^{n-1} x[k]}{\tau} = \mathrm{x[n]} - \left(1 - \frac{1}{\tau}\right)\mathrm{x[n-1]} + \mathrm{A[n-1]}. \quad (3)$$

The deconvolution equation reshapes the exponential pulse into a staircase signal. To measure the height of the step signal one should differentiate the deconvulated signal. By applying the numerical differentiation, the MWD equation with a window M is obtained [3]:

$$MWD_M[n] = A[n] - A[n-M] = x[n] - x[n-M] + \frac{1}{\tau}\sum_{k=n-M}^{n-1} x[k]. \quad (4)$$

The MWD algorithm converts an exponentially decaying signal into a step signal with length M. However, at this point the signal to noise ratio is not yet improven. To impove the signal to noise ratio, a low pass filter is applied after the MWD module, implemented as a moving window averager. In the MWD algorithm the shaped pulse is a trapezoid which emerges as a convolution sum of the digitized signal with a kernel function. After the MWD processing the signals with good statistics and well-defined exponential shape transform into trapezoids. However, the signals with bad statistics, 'noised exponential shape' convert into the 'noised' trapezoids with the statistical fluctuations on the trapezoid tails (see figure 1). These statistical fluctuations may produce false triggers.

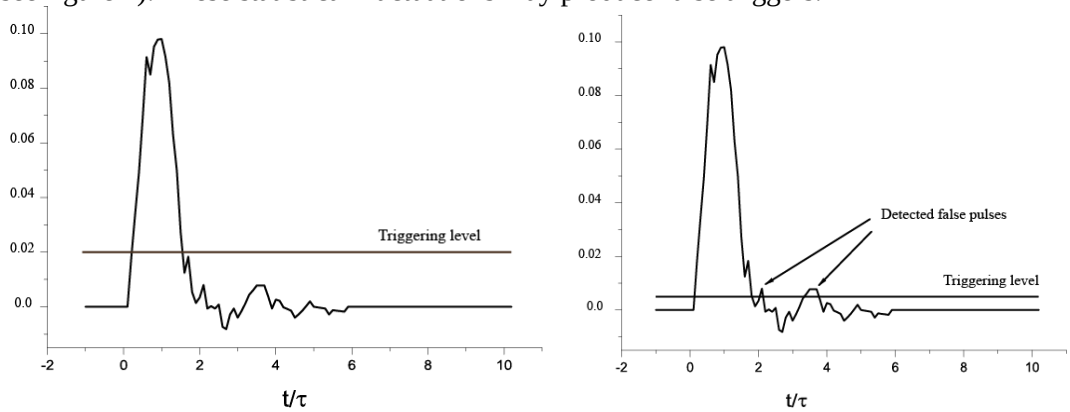

Figure 1. The simulated signal processed with the MWD algorithm. Left :The example of a high threshold. Right: The example of a low threshold.

2. The adaptive triggering method

The problem of the 'noised' pulse tails is solved at the time with the two approaches. The first one is to raise the trigger threshold above the fluctuations level. The second one is to introduce a deadtime after

each pulse. However, both methods have their shortcomings. The low triggering level causes the detection of false pulses (see figure 1). On the other hand, with increasing triggering level above the fluctuation level, the false pulses will not be detected. However, the pulses which amplitudes are below the triggering level are also not detected and therefore the dynamic range of the detector is lowered (see figure 1). The second approach is to introduce a deadtime after each pulse. This approach can work fairly well at low count rates but at high count rates this approach becomes inefficient. Closely separated pulses get rejected, which manifests with a lower detection efficiency.

We propose a new method with an aim to improve the signal processing. The proposed method is the adaptive triggering for scintillation signals (see figure 2). In our metod the trigger is raised by a finite value and for a finite amount of time after each pulse. Namely, after the detected pulse, the threshold is set to a low level. Immediately after the pulse is detected the threshold is raised by a finite value and for a finite value of time. After a finite value of time the threshold is lowered to the previous value. In this way the afterpulses which occur immediately after the detected pulse are not detected (It should also be noted that the probability of the ocurrence of this pulses decreases with a time from the real pulse due the their stohastic nature). At the same time the small pulses that precede or follow the real pulse can be detected.

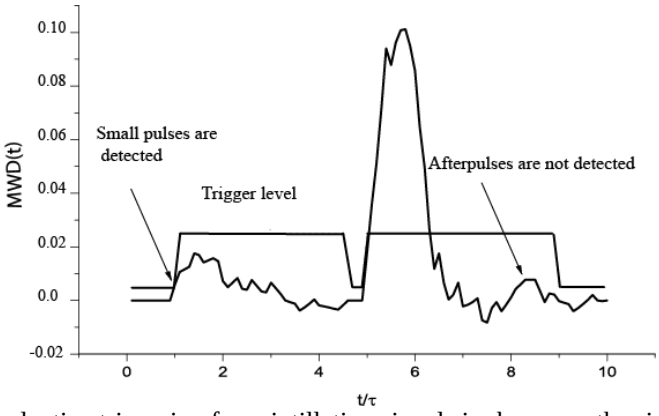

Figure 2. The method of adaptive triggering for scintillation signals is shown on the simulated signal. The small pulses are detected, while the afterpulses are not detected.

In order to determine the adaptive triggering parameters (the value and the time for which the trigger is raised) and in order to test our method, we firstly simulated the simple signals. The energy spectrum of the simulated signal is given as:

$$\frac{1}{N_0}\frac{dN(E)}{dE} = \frac{1}{2}\big(c\delta(E-E_1) + (1-c)\delta(E-E_2)\big), c = \frac{N_1}{N_o}, \quad (5)$$

where N is a total number of incident particles, and N_1 and N_2 represent the number of particles with energies E_1 and E_2, respectively.

As about the simulation parameters, for the beam frequency we chose the value of 10^5 Hz. For the decay time the value of 250 ns (which is fairly close to the decay time of the NaI(Tl) used in our experiment) was used. Our reference energy excited 1000 states, and for the bandwidth of energy histograms we choose the value of 200 MHz. The latter value corresponds to the bandwidth of the real measuring systems. The ideal energy spectrum should consists of two infinitely narrow peaks. Due to the finite precision of the simulated algorithm we expect the energy peaks to broaden. Also due to the afterpulses, we expect to have an increased low energy background. Due to the real pulses that appear immediately after the afterpulses (and therefore the concluded information about their amplitude is wrong) we also expect to have some background counts between the peaks.

As a criterion for determining the optimal triggering parameters we chose the relative number of low energy background counts, since this value strongly depends on the triggering parameters. For the optimal parameters we chose the values that after increasing do not decrease the relative number of background counts. Afterwards, the obtained optimal parameters for different energies were tested with the other simulated signal with simple energy spectrum given as:

$$h_{ideal}(\mathrm{E}) = \frac{1}{N_0}\frac{dN(E)}{dE} = \begin{cases} \frac{1}{E_1}, E < E_1 \\ 0, E > E_1 \end{cases}, \quad (6)$$

The same MWD parameters were used as in a previous case. The quality of parameters was deduced using a chi square method [4]:

$$\sigma_{spect} = \left(\frac{1}{n-1}\sum_{i=1}^{n}(h(E_i) - h_{ideal}(E_i))^2\right)^{1/2}, \quad (7)$$

where $h(E_i)$ denotes the measured value and $h_{ideal}(E_i)$ the correct value.

We employed the adaptive triggering by choosing the optimal parameters for the value and the time for which the trigger is raised, for every simulated pulse. As it can be seen from figure 3, the difference between the constant threshold and the adaptive triggering method is mostly pronounced at the lowest energies. With the constant threshold we basically lost the information about the low energy part of the spectrum, while with the adaptive triggering method this information is retained.

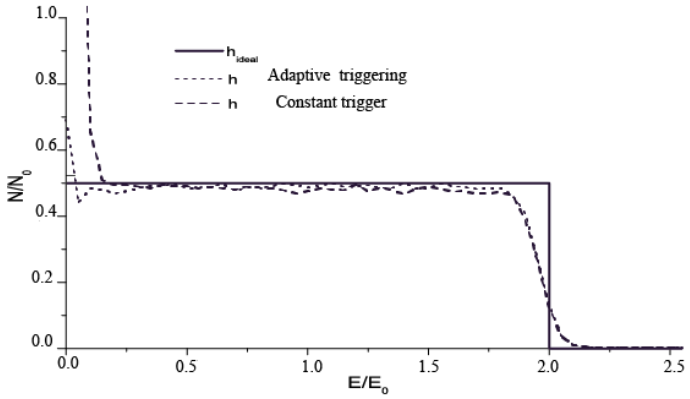

Figure 3. The energy spectrum given with eq. 7. The constant triggering (dashed line) and adaptive triggering method (dotted line) were employed.

In order to test the simulation parameters, we performed a simple experiment. As a radiation source ^{137}Cs was used. For the gamma ray detection NaI(Tl) scintillator coupled to a Photonis PMT was used. Raw anode output signal was sampled with a PicoScope digitizer with a sampling period of 200 ps and a resolution of 8 Bits. Two experimental setups were performed, by varying the distance of the source from the detection system. The one with a smaller pulse frequency was used as a reference measurement (i.e. for calibration, etc).

The obtained spectrum with employed constant threshold method is shown on figure 4. The K_α X-ray line from Ba [5] (decay product of ^{137}Cs) is not visible in the spectrum since the low energy part of the spectrum is noised up with the false pulses. With increasing the threshold the background lowers, however the dynamic range of the detectors lowers as well. Also, it can be noticed that the peak with energy approximately equal to the threshold energy is also detected. The peak is the consequence of the fact that the afterpulses are mainly detected at the energy near to the threshold energy.

The obtained spectrum with the adaptive threshold trigerring method is shown at figure 5. For the low values of the adaptive threshold, low energy peak is piled up with the afterpulses. For the higher values of the adaptive threshold, the low energy peak is clearly visible. However, also false peak with energy approximately equal to the constant threshold plus adaptive threshold can be noticed, as well. This peak is as in a previous case the consequence of the fact that the afterpulses are mainly detected at energy near to the threshold energy.

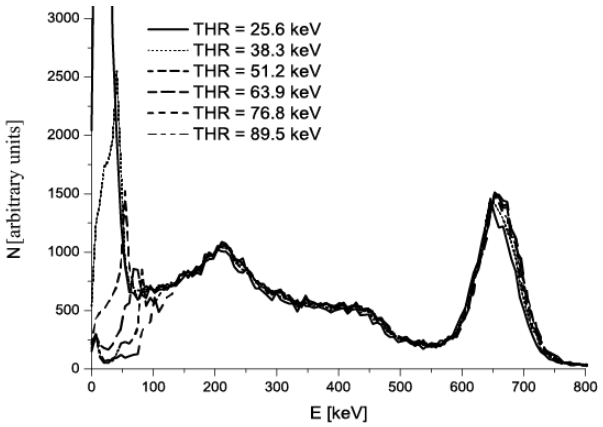

Figure 4.The obtained energy spectrum for different values of the constant threshold THR.

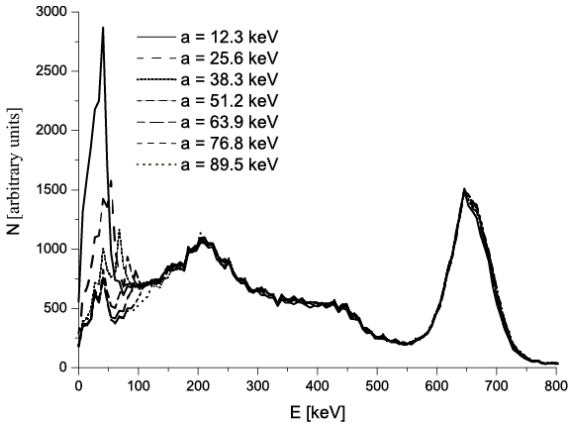

Figure 5 .The obtained energy spectrum for different values of the adaptive threshold a.

3. Conclusions

To conclude, we propose a new method for the signal processing. In our method, the trigger is raised by a finite value and for a finite amount of time after each pulse. The method was first tested on simple simulated signals. Consequently, based on the simulation results, the optimal triggering parameters were obtained. Using these parameters, adaptive triggering was then tested with a NaI(Tl) detector in an intense ^{137}Cs gamma-ray field. The results show that this method significantly extends the useful energy range on the low energy side of the spectrum when post-pulse inhibition is not applicable due to high count rates. This is crucial if the desired information is present there.
Last but not least, we have to state that our method is still in the development phase, more complicated synthetised signals should certainly be studied as well as the dependence of this method on the MWD parameters and initial pulse frequency.

4. References

[1] G.F. Knoll, Radiation Detection and Measurement, John Wiley & Sons, New York, (2000).

[2] H. Yang, D. K. Wehe, D. M. Bartels, Nucl. Instrum. Meth. A, **598**, 779 (2009).
[3] A. Georgiev, W. Gast R. M. Lieder, IEEE Trans. Nucl. Sci. 41, 1116 (1994).
[4] W. R. Leo, Techniques for Nuclear and Particle Physics Experiments, Springer, 1994.
[5] E. Browne, J. K. Tuli, Nuclear Data Sheets 108, 2173 (2007).

J. V. is grateful to European Social Fund and Republic of Slovenia, Ministry of Education, Science and Sport for financial support.